Hydrol. Earth Syst. Sci. Discuss., 10, 7537–7574, 2013
www.hydrol-earth-syst-sci-discuss.net/10/7537/2013/
doi:10.5194/hessd-10-7537-2013

Hydrology and Earth System Sciences
Discussions
Open Access

Analysis of groundwater drought using a variant of the Standardised Precipitation Index

J. P. Bloomfield[1] **and B. P. Marchant**[2]

[1]British Geological Survey, Maclean Building, Crowmarsh Gifford, Wallingford, Oxfordshire, OX10 8BB, UK
[2]British Geological Survey, Environmental Science Centre, Keyworth, Nottingham, NG12 5GG, UK

Received: 21 May 2013 – Accepted: 3 June 2013 – Published: 14 June 2013

Correspondence to: J. P. Bloomfield (jpb@bgs.ac.uk)

Published by Copernicus Publications on behalf of the European Geosciences Union.

Abstract

A new index for standardising groundwater level time series and characterising groundwater droughts, the Standardised Groundwater level Index (SGI), is described. The SGI is a modification of the Standardised Precipitation Index (SPI) that accounts for differences in the form and characteristics of precipitation and groundwater level time series. The SGI is estimated using a non-parametric normal scores transform of groundwater level data for each calendar month. These monthly estimates are then merged to form a continuous index. The SGI has been calculated for 14 relatively long, up to 103 yr, groundwater level hydrographs from a variety of aquifers and compared with SPI for the same sites. The SPI accumulation period which leads to the strongest correlation between SPI and SGI, q_{max}, varies between sites. There is a positive linear correlation between q_{max} and a measure of the range of significant autocorrelation in the SGI series, m_{max}. For each site the strongest correlation between SPI and SGI is in the range 0.7 to 0.87, and periods of low values of SGI coincide with previously independently documented droughts. Hence SGI is taken to be a robust and meaningful index of groundwater drought. The maximum length of groundwater droughts defined by SGI is an increasing function of m_{max}, meaning that relatively long groundwater droughts are generally more prevalent at sites where SGI has a relatively long autocorrelation range. Based on correlations between m_{max}, average unsaturated zone thickness and aquifer hydraulic diffusivity, the source of autocorrelation in SGI is inferred to be dependent on aquifer flow and storage characteristics. For fractured aquifers, such as the Cretaceous Chalk, autocorrelation in SGI is inferred to be primarily related to autocorrelation in the recharge time series, while in granular aquifers, such as the Permo-Triassic Sandstones, autocorrelation in SGI is inferred to be primarily a function of intrinsic aquifer characteristics. These results highlight the need to take into account the hydrogeological context of groundwater monitoring sites when designing and interpreting data from groundwater drought monitoring networks.

HESSD

10, 7537–7574, 2013

Analysis of groundwater drought using a variant of SPI

J. P. Bloomfield and B. P. Marchant

1 Introduction

Drought is a costly natural hazard affecting socio-economic activity and agricultural livelihoods as well as adversely impacting public health, and threatening the sustainability of many natural environments (Wilhite, 2000; Fink et al., 2004; Sheffield and Wood, 2008; Calow et al., 2010; Mishra and Singh, 2010). Droughts typically develop slowly and can last from months to a few years (Santos, 1983; Lloyd-Hughes and Saunders, 2002; Tallaksen and van Lanen, 2004; Tallaksen et al., 2009). As highlighted in a recent review of drought concepts by Mishra and Singh (2010), groundwater droughts are of particular interest due to the manner in which drought propagates through hydrological systems. During the early stages of a drought, as deficits are developing in surface water and unsaturated zone stores, groundwater sources can provide relatively resilient water supplies and will sustain surface flows through groundwater baseflow (Hughes et al., 2012). Conversely, groundwater may be highly susceptible to relatively persistent or prolonged droughts, because, compared with surface water resources, groundwater storage may take significantly longer to be replenished and recover as a drought begins to break.

A number of studies have sought to develop a better understanding of groundwater droughts in the context of meteorological drivers and, in particular, how droughts propagate through hydrological systems (Eltahir and Yeh, 1999; Peters et al., 2003, 2005, 2006; Tallaksen et al., 2006, 2009; van Lanen and Tallaksen, 2007; Leblanc et al., 2009). These studies have usually focussed on the catchment scale and have brought process understanding to bear on the evolution of groundwater droughts. Fewer studies have concentrated on regional characterisation of groundwater droughts, emphasising monitoring, characterisation of longer-term trends and the development of drought warning systems (Chang and Teoh, 1995; Bhuiyan et al., 2006; Mendicino et al., 2008; Fiorillo and Guadagno, 2010, 2012). A common feature of these latter studies is the need to develop relatively simple but consistent measures or indices of the status of groundwater drought: indices that can be applied between different observation sites,

HESSD
10, 7537–7574, 2013

J. P. Bloomfield and B. P. Marchant

aquifers and catchments at the regional scale, as well as that enable groundwater drought to be compared with other hydro-meteorological aspects of drought. Despite the previous work, there are still no commonly accepted indices to quantify groundwater droughts, so making it difficult to incorporate groundwater drought phenomena into wider drought assessments. To address this shortcoming, here we present for the first time a systematic assessment of how one of the most commonly used hydrological drought indices, the Standardised Precipitation Index (SPI), can be applied to groundwater level data in order to define a new groundwater level index for use in groundwater drought monitoring and analysis.

Context for development of the SGI

Many drought indices have been developed in recent decades to enable drought severity, duration and spatial extent to be characterised and compared in a standardised manner (Panu and Sharma, 2000; Mishra and Singh, 2010). Mishra and Singh (2010) provide a commentary on the strengths and weaknesses of a number of these indices as well as on their comparative performance. One of the most widely used indices is the SPI, (McKee et al., 1993; Edwards and McKee, 1997). The SPI was originally developed as a simple method for characterising meteorological drought. It consists of a normalised index obtained by fitting a parametric distribution function to long-term precipitation records and is calculated for a range of rainfall accumulation periods or time scales. As noted by McKee et al. (1993), it is potentially applicable to any hydrometric series, including groundwater levels, which reflects changes in the state of water resources. Consequently, variants of the SPI methodology have been applied to other aspects of the hydrological system such as surface flows, reservoir storage and soil moisture (e.g. Vincente-Serrano and Lopez-Moreno, 2005; Shukla and Wood, 2008; Nalbantis and Tsakiris, 2009;) as well as studies of groundwater droughts (Bhuiyan et al., 2006; Fiorillo and Guadagno, 2010, 2012). The method has recently been extended to include atmospheric water demand (Vincente-Serrano et al., 2010; McEvoy et al., 2012).

Deployable output from water supply boreholes is a function of groundwater level. Hence, if an appropriate standardised index can be applied, groundwater levels at observation boreholes are a useful measure of the quantitative status of groundwater resources during a regional drought. As will be shown, differences in the form and characteristics of the different types of hydrometric time series require modifications to be made to the SPI methodology of McKee (McKee et al., 1993; Edwards and McKee, 1997) if the methodology is to be applied to groundwater level hydrographs and so to the analysis of groundwater droughts. In this paper issues related to the application of the SPI to groundwater level time series are addressed, and a modification to the SPI methodology is presented that enables monthly groundwater level time series to be used as the basis for estimating a new Standardised Groundwater level Index (SGI). The SGI is calculated for groundwater level hydrographs from 14 sites across the United Kingdom (UK), where sites have been selected from a range of aquifer types and to exhibit a range of hydrograph characteristics. The relationships between SPI and SGI at the study sites are investigated and quantified using correlation analysis. Groundwater droughts at the study sites are then identified and described using the SGI time series and the influence of some possible hydrogeological explanatory factors on SGI is explored.

2 Study sites and data

Groundwater level hydrographs from 14 sites across the UK have been used in the study. The sites are part of the UKs long-term observation borehole network, consist of a broad range of unconfined consolidated aquifers types and are not significantly affected by pumping (Bloomfield et al., 2009). The sites include those located on the Lincolnshire Limestone, a fractured limestone aquifer (Allen et al., 1997); the Chalk aquifer, a dual porosity, dual permeability carbonate aquifer with local karstic development (Bloomfield, 1996; Maurice et al., 2006); and the Permo-Triassic Sandstone and Lower Greensand aquifers (Allen et al., 1997; Bloomfield et al., 2001) where inter-

HESSD
10, 7537–7574, 2013

Title Page
Abstract | Introduction
Conclusions | References
Tables | Figures
◀ | ▶
◀ | ▶
Back | Close
Full Screen / Esc
Printer-friendly Version
Interactive Discussion

grannular flow predominates. Figure 1 shows the location of the observation boreholes in relation to the major aquifers in the UK, and summary information about the sites and groundwater hydrographs is given in Table 1, where all groundwater levels in Table 1 and subsequent figures is reported as metres above mean sea level.

Monthly groundwater level data for the study sites has been taken from the UK National Groundwater Level Archive (National Groundwater Level Archive, 2013). The monthly groundwater level records range in length from 29 to 103 yr. Figure 2 is a plot of the monthly groundwater level hydrographs for the 14 sites, where all hydrographs are drawn to the same scale. Precipitation data has been derived from two sources. For 1961 to the end of 2005 precipitation data is taken from the Centre for Ecology and Hydrology's CERF 1 km gridded precipitation dataset (Keller et al., 2005). Pre-1961 monthly precipitation data has been taken from the Meteorological Office Integrated Data Archive System, MIDAS (BADC, 2013). The rainfall records are combined to give a continuous precipitation record at each site. An example of a precipitation time series is given in Fig. 3. It shows one month accumulated precipitation for Dalton Holme plotted with the corresponding monthly groundwater level. Average annual precipitation varies between sites from 580 to 1100 mm (Table 1).

3 Statistical methods

3.1 Development of a new Standardized Groundwater Index (SGI)

The SPI was proposed by McKee et al. (1993) as an objective precipitation-based measure of the severity and duration of droughts. McKee et al. (1993) suggested that drought status could be described by a normally distributed index. The index was fitted to a time series of the recorded precipitation at a site for accumulation periods of 3, 6, 12, 24 and 48 months. The calculation of the SPI requires three steps. First a gamma distribution is fitted to the time series of accumulated precipitation observed at a particular site. The precipitation time series is denoted z_i for $i = 1, 2, \ldots, n$ where

HESSD
10, 7537–7574, 2013

i is the number of months since the start of the time series and n is the total number of observations. For each $i = 1,2,\ldots,n$, McKee et al. (1993) then used the fitted distribution to determine p_i, the probability that a value drawn at random from the fitted distribution was less than or equal to z_i. Finally McKee et al. (1993) applied the inverse normal cumulative distribution function (with mean zero and variance one) to these p_i to yield a length n time series of SPI values denoted here as $\mathrm{SPI}_q(i)$, where q is the number of months over which rainfall is accumulated. The resulting SPI is a continuous variable, however, McKee et al. (1993) also arbitrarily defined drought intensity according to the SPI where they denoted SPI ≤ -2 corresponding to extreme drought, $-1.5 \geq \mathrm{SPI} > -2$ corresponding to severe drought, $-1.0 \geq \mathrm{SPI} > -1.5$ corresponding to moderate drought, $0 \geq \mathrm{SPI} > -1$ corresponding to minor drought and $\mathrm{SPI} > 0$ corresponding to no drought.

It would be possible to calculate a Standardized Groundwater Index (SGI) by exactly the same method using monthly groundwater levels instead of accumulated precipitation. However, some differences between observed groundwater level hydrographs and precipitation time series should be borne in mind. Firstly, groundwater level is a continuous variable and there is no need to accumulate it over a specified time period. Secondly, a much stronger seasonal pattern of variation is evident in UK groundwater levels than is seen in accumulated precipitation values (Fig. 3). If the SPI methodology were naively followed using such strongly seasonal data then the resultant SGI may appear to include regular droughts each summer and therefore this seasonal trend must be removed from the data prior to calculation of a meaningful SGI. This could be achieved by fitting a periodic model of the annual variation in groundwater levels. The SGI, however, may still be unduly influenced by deviations of the data from a simple periodic model and a more effective way to remove the seasonal effect is to estimate the SGI separately for each calendar month and then merge the resulting SGIs to form a continuous time series. Even when any seasonal trend has been removed, the distributions of observed groundwater levels may be irregular. For example, Fig. 4 (left panels) shows four histograms of observed groundwater levels for particular calendar

HESSD
10, 7537–7574, 2013

months at four of the study sites – (a) Chilgrove House in November, (c) New Red Lion in April, (e) Therfield Rectory in May and (g) West Dean No. 3 in June. The four histograms differ in the sign and magnitude of their skewness. Therefore distribution functions which can represent more general behaviour than the gamma distribution are required to model variations in the form of monthly distributions of groundwater levels.

We initially fitted normal, log-normal, gamma and extreme-value distributions to the monthly groundwater levels at each site by maximum likelihood (MATLAB, 2012). These distributions were selected because they can accommodate all magnitudes of non-negative skewness from zero to severe. Negative skewness was accommodated by applying a shift $z_i^* = c - z_i$ for constant c to the data prior to fitting the distribution. Figure 4 (left panels) shows the best-fitting distribution functions according to the Akaike information criterion (Akaike, 1973) for the four example histograms and the corresponding plots on the right show the SGI which results. The best-fitting distribution function is different in each case. For Chilgrove House in November it is the gamma distribution. For New Red Lion in April it is the negatively skewed extreme value distribution and for Therfield Rectory in May and West Dean No. 3 in June it is the log-normal and extreme value distributions respectively. Figure 4 (right panels) shows that the quality of the computed SGIs also appears to vary in regards to how well the estimated values of SGI correspond to the normal distribution of zero mean and standard deviation of one. The quality of the estimated values of SGI for all months at all 14 sites have been estimated by applying the Kolmogorv–Smirnov test for normality (Everitt, 2002). The results are highly variable, with one distribution of SGI, for Chilgrove House in November, failing the K–S test at the $p = 0.05$ level. Given the variation in the degree to which these SGI estimated from parametric models conform to the normal distribution it is doubtful whether they can be objectively compared.

An alternative approach to fitting standardized distributions is to apply the normal scores transform (Everitt, 2002). This is a non-parametric normalization of data that assigns a value to observations, in this case monthly groundwater levels, based on

HESSD
10, 7537–7574, 2013

Analysis of groundwater drought using a variant of SPI

J. P. Bloomfield and B. P. Marchant

their rank within a dataset, in this case groundwater levels for a given month from a given hydrograph. We note that a related non-parametric method, the plotting position method, has previously been used by Osit et al. (2008) to estimate standardised precipitation for comparison with SPI. The normal scores transform is undertaken by applying the inverse normal cumulative distribution function to n equally spaced p_i values ranging from $1/2n$ to $1-1/2n$. The values that result are the SGI values. They are then re-ordered such that the largest SGI value is assigned to the i for which p_i is largest, the second largest SGI value is assigned to the i for which p_i is second largest and so on. The SGI distribution which results from this transform will always pass the K–S normality test.

In some statistical applications it is undesirable to use a normal scores transform because the model is over-fitted. This means that the model matches the particular intricacies of the existing observed data to a degree that will not be achieved on independently gathered observations of the same property. This could mean that the uncertainty of a prediction of the property at a time when it was not measured is under-estimated. However, we wish to use the normal scores data to describe existing observations rather than to predict values. Therefore we need not be concerned by over-fitting even if it is present for some of the normal scores transforms.

In summary, for each of the 14 study sites, normalized indices are estimated from the groundwater level data for each calendar month using the normal scores transform. These normalized indices are then merged to form a continuous SGI. The SPI is estimated directly for the entire time series rather than splitting the series into calendar months. At each site SPI is estimated with accumulation periods of $1, 2, \ldots, 24$ months. To ensure consistency between groundwater and precipitation indices SPIs are also estimated using the normal scores transform.

HESSD
10, 7537–7574, 2013

3.2 Methods used to analyse SGI, correlations with SPI and hydrogeological factors influencing the drought indices

In order to quantify groundwater droughts using the SGI, we are interested in characterising the autocorrelation in SGI time series. Autocorrelation can be quantified using a correlogram (Diggle, 1990). If we denote the mean SGI for the borehole by $\overline{\mathrm{SGI}}$ then the k-th sample autocovariance coefficient is defined to be

$$g_k = \frac{1}{n} \sum_{i=k+1}^{n} \left\{ \mathrm{SGI}(i) - \overline{\mathrm{SGI}} \right\} \left\{ \mathrm{SGI}(i-k) - \overline{\mathrm{SGI}} \right\} \quad (1)$$

and the k-th sample autocorrelation coefficient is

$$r_k = \frac{g_k}{g_0}. \quad (2)$$

The correlogram is a plot of r_k against k. If there is no correlation between the SGI(i) observed k months apart and if the SGI values are normally distributed then r_k is approximately normally distributed with mean zero and variance $1/n$. Therefore values of r_k with magnitude greater than $2/\sqrt{n}$ suggest significant correlation at approximately the 5 % level. We define the range of significant temporal correlation for a SGI to be the largest m, $m_{\max}$, for which $r_k > 2/\sqrt{n}$ for all $k \leq m$. The threshold on the autocorrelation coefficients which signifies significant correlation will vary according to the length of the time series. Since we wish to use a common threshold for all of our SGI series to enable comparison between sites we have selected 0.11 as the SGI autocorrelation threshold, t_{SGI}, since this is the significant threshold ($p = 0.05$) for our shortest SGI time series (for Lower Barn Cottage with a record length of 29 yr).

In addition, linear correlation coefficients have also been calculated to quantify the strength of relationships between SPI and SGI, and between $m_{\max}$ and possible explanatory variables. These explanatory variables, including unsaturated zone thickness, aquifer transmissivity (T) and storage coefficients (S) and hydraulic diffusivity

HESSD
10, 7537–7574, 2013

(T/S) have been estimated for each site and are listed in Table 1. Note that no pumping test data is available for any of the study sites, so T and S values are estimates based on mean values derived from pumping tests for a given region and aquifer combination as reported by Allen et al. (1997). An exception is that unconfined storage coefficients for sites on the Permo-Trias sandstone aquifer are estimated to be 0.1 (also after Allen et al., 1997). This is because, as Allen et al. (1997) note, estimates of S from short-term pumping tests on this aquifer typically significantly underestimate long-term storage and a value of 0.1 for S has been taken as the optimal value for long-term storage.

4 Results

4.1 Estimated SGI and SPI

Estimated monthly SGI for each of the 14 study sites are given in Fig. 5. In the present study SPI has been estimated for $q = 1, 2, \ldots, 24$ months. However, SPI is usually only calculated and reported for selected periods. So for simplicity and to illustrate how SPI varies with q at one of the study sites, Fig. 6 shows SPI for Dalton Holme for $q = 1$, 3, 6, 12 and 24 months. Figure 6 also includes the SGI time series for Dalton Holme for comparison with the SPI time series.

Compared with the raw groundwater level data, Fig. 2, the SGI data does not contain a strong seasonal component, Fig. 5, and unlike the groundwater level time series, the SGI time series show many similar broad-scale structures across all the sites. For example, all sites show generally low values of SGI in the early 1990s, with SGI increasing in the mid-1990s and then decreasing again in the later 1990s. There are, however, differences in the short-range variation in SGI between sites. For example, the SGI for Ashton Farm, Chilgrove House and West Dean No. 3 appear to be considerably noisier than Therfield Rectory, Stonor Park or Llanfair DC. This reflects differences in the structure of the SGI autocorrelation between the sites. Figure 7 (middle panels) shows

HESSD
10, 7537–7574, 2013

plots of SGI autocorrelation as a function of lag in months (solid lines) for three example sites, Ashton Farm, Dalton Holme and Llanfair DC, with contrasting autocorrelation. Using the SGI autocorrelation threshold, t_{SGI}, of 0.11 (the dashed line in the figure), the SGI autocorrelation range ($m_{\max}$) for each of the sites has been estimated and is given in Table 2. Table 2 shows that significant temporal autocorrelation in SGI, $m_{\max}$, varies between sites, from as little as 4 months at Ashton Farm up to 28 months at Llanfair DC.

As has been noted by McKee et al. (1993) and in previous studies (Vincente-Serrano and Lopez-Moreno, 2005), the degree of noise or short-range variation in SPI varies as a function of the precipitation accumulation period. This is also seen in the present study. For example, the SPI for Dalton Holme is relatively noisy when $q = 1$ compared with SGI Fig. 6, and Fig. 7 (middle panels) shows the very short autocorrelation range for SPI ($q = 1$) at the three example sites. However, SPI becomes smoother and less noisy and long-range correlations become more prominent as precipitation accumulation periods increase, Fig. 6.

4.2 Correlation between SPI and SGI

The cross-correlation between SPI and SGI for SPI accumulation periods of $q = 1, 2, \ldots, 24$ has been computed and is shown for three representative sites in Fig. 7 (bottom panels). At each site a maximum correlation associated with an optimum SPI accumulation period can be identified and is denoted by an X on each of the cross-correlation curves. However, investigation of the cross-correlation co-efficients for a range of lags between SPI and SGI shows that the maximum correlation may not necessarily occur at a lag of zero months. So for all sites the cross-correlation between SPI and SGI has been estimated for SPI accumulation periods of $q = 1, 2, \ldots, 24$ months and for lags of one month increments up to 24 months. The resulting cross-correlations are presented in the form of a heat map, Fig. 8, where dark blue tones denote weaker correlations and dark red tones denote stronger correlations, and where the maximum correlation is marked by the black square. Generally the maximum correlation is as-

HESSD
10, 7537–7574, 2013

J. P. Bloomfield and B. P. Marchant

sociated with lag zero, however, at Little Bucket Farm, Therfield Rectory and Stonor, the maximum correlation is associated with lags of 1, 1, and 2 months respectively. Table 2 lists the values of the maximum cross-correlation between SPI and SGI, as well as associated the accumulation period (q_{max}) and associated lag. The maximum cross-correlations between SPI and SGI are generally strong with coefficients typically in the range 0.7 to 0.87, Table 2, with the highest coefficient of 0.87 associated with the site at Little Bucket Farm and the lowest coefficients of 0.7 associated with the site at West Dean No. 3 – both sites being on the Chalk aquifer. Plots of SGI as a function of SPI q_{max} show that for all sites there is a linear relationship between the two drought indices, Fig. 9.

The SPI accumulation period associated with the maximum cross-correlations, q_{max}, and the SGI autocorrelation range, m_{max}, both vary between sites and broadly increase in the same order for the study sites. When q_{max} is plotted against m_{max}, Fig. 10, there is an approximate one-to-one relationship with correlation coefficient of 0.79 that is significant for $p < 0.001$.

4.3 Groundwater droughts as defined by SGI

Cole and Marsh (2006) and Marsh et al. (2007) identified seven episodes of major droughts in England and Wales during the period covered by the groundwater level records investigated in the present study. They noted that all the droughts had large geographical footprints extending over much of England and Wales and in some cases affecting the whole of the UK, but that regional variations in drought intensities are present within and between the major drought events. Of these major droughts, they estimated that all but one had sustained and or severe impacts on groundwater levels. Marsh et al. (2007) also noted that a number of the droughts were characterised by transitions from initial surface water stress to lowered groundwater heads at the national and regional scales. Table 3 (after Marsh et al., 2007 and National River Flow Archive, 2013) summarises the major droughts in England from 1900 to the end of 2005, the period covered by the groundwater level records used in the present study,

HESSD
10, 7537–7574, 2013

and includes a brief commentary after Marsh et al. (2007) on the individual drought characteristics.

Figure 11 is a re-presentation of the SGI data from Fig. 5 as a heat map, where non-drought periods, SGI > 0, are shown in grey, and drought periods, SGI < 0, are shown in shades of yellow through to red with decreasing SGI, i.e. with increasing drought intensity. Figure 11 is consistent with the observations of Marsh et al. (2007) that the UK has experienced a number of major groundwater droughts. In particular, the droughts of 1976, 1990 to1992, and 1995 to 1997 are clearly expressed by the SGI records at the majority of sites. Groundwater droughts prior to the early 1970's are less easy to discern as there are fewer records. In addition, the following specific observations can be made:

- There is no evidence in the SGI data to support a significant groundwater component to the 1959 drought episode, however, this is consistent with the observation of Marsh et al. (2007) that this drought had modest groundwater impact.
- The 1933–1934 drought episode appears prominently in the SGI records at Chilgrove House, but is absent from the record at Dalton Holme suggesting that it may have been less significant in the northern part of the region.
- The 1921–1922 drought episodes appear in the SGI records at both Chilgrove House, and Dalton Holme.
- There is some evidence from the Chilgrove House record for short drought episodes between 1900 and 1910 as part of the 1890–1910 "Long Drought".
- In addition, the SGI records indicate that groundwater drought conditions not previously identified by Marsh et al. (2007) were experienced at a number of sites during the mid-1960s, and the mid- and late 1940s.

Based on these observations, SGI appears to record groundwater drought response to hydro-meteorological droughts previously documented by Marsh et al. (2007) as well

HESSD
10, 7537–7574, 2013

J. P. Bloomfield and B. P. Marchant

as adding apparent refinements to the drought history. Figure 11 is also consistent with the assertion of Marsh et al. (2007) that many of the hydrometric droughts in England and Wales have a wide geographic impact. Sites at the geographical extent of the study area, such as Dalton Holme in the northeast, Llanfair DC in the northwest, Bussels No. 7 in the southwest, and Little Bucket Farm in the southeast, all record drought events in the form of anomalously low SGI values for the droughts of 1976, 1990 to 1992 and 1995 to 1997.

5 Discussion

The SGI autocorrelation varies significantly between sites, but given that one of the purposes of developing a groundwater drought index is to compare standardised measures of drought between sites, what are the implications, if any, of this observation? For example, it may be expected that the autocorrelation structure of SGI will influence the length of groundwater droughts recorded at a given site, where sites with relatively long significant SGI autocorrelations might experience a limited number of relatively long droughts and sites with relatively short significant SGI autocorrelations may experience more numerous but briefer episodes of groundwater drought. How does $m_{\max}$ influence temporal patterns of groundwater drought at a site, and if $m_{\max}$ influences groundwater drought response, what are the possible causes of or controls on $m_{\max}$?

5.1 The relationship between $m_{\max}$ and drought duration

To investigate the effect of autocorrelation in SGI on groundwater drought, here we assume that, as a first-order approximation, the broad meteorological drought history of the study sites is spatially homogeneous and investigate how drought duration defined by SGI varies between sites as a function of $m_{\max}$. This assumption means that any comparative differences in drought characteristics between sites would need to be explained in terms of intrinsic differences in the SGI time series, rather than differences in

HESSD
10, 7537–7574, 2013

the drought climatology. This assumption has been justified on the grounds that Marsh et al. (2007) noted that all the major hydrological drought episodes in England and Wales affected "almost all of the UK", i.e. covering an area significantly greater than that defined by the sites used in the current study. In addition, recent studies of the spatial coherence of hydrological droughts in the UK (Hannaford et al., 2010; Fleig et al., 2011) indicate that the current study sites fall within a homogeneous drought region ("region 4" of Hannaford et al., 2010, and "region GB3" of Fleig et al., 2012). Notwithstanding the assumption of drought homogeneity, it is noted that any comparison between sites will be at best semi-quantitative due to the varying lengths of records. Wu et al., 2005 have previously cautioned against quantitative comparisons of SPI series for different sites that are based on different length records. Consequently, using the SGI time series presented in Fig. 11, only simple measures of drought duration, i.e. median and maximum duration, have been estimated for each site, rather than undertaking a complete frequency analysis of drought durations. Here drought duration is taken to be a period where monthly SGI is continuously negative at a site.

Median and maximum drought durations are given in Table 2. Median durations range from 2 months at Lower Barn Farm and West Dean No. 3 to 11 months at Well House Inn, and maximum durations range from 12 months at Ashton Farm to 71 months at Llanfair DC respectively. The median drought duration appears to be insensitive to m_{max}, however, as postulated, maximum drought duration is broadly positively correlated with m_{max}, Fig. 12 (left panel). It should be noted though that although the converse is true, that sites with short m_{max} generally have shorter maximum drought durations, such sites may still respond to and record major drought episodes. For example, Ashton Farm and Chilgrove House which have two of the shortest m_{max} (4 and 6 months respectively) both had low values of SGI during the 1976 drought and had an increased frequency of low values of SGI during the 1990–1992 drought event, Fig. 11, though in the case of this latter drought low monthly SGI values were interspersed with months of positive non-drought SGI. The positive correlation of maximum drought duration with m_{max} is particularly evident for the Permo-Trias sandstone

HESSD
10, 7537–7574, 2013

aquifer sites, Bussels No. 7, Heathlanes and Llanfair DC, which have m_{max} values of 19, 24 and 28 months and maximum drought durations of 40, 64 and 71 months respectively despite being some of the shortest SGI records, Fig. 12 (left panel). The longest droughts at these sites are associated with but extend beyond the 1990–1992 drought event, Fig. 11. There appears to be some association between aquifer type and the relationship between maximum drought duration and m_{max}, Fig. 12 (left panel). For a given maximum drought length, the Chalk sites tend to have slightly lower m_{max} compared with the sites on the Permo-Trias sandstone and it can be inferred from this observation that aquifer specific factors may influence both SGI autocorrelation and drought histories at a given site.

5.2 Evidence for hydrogeological controls on m_{max}

In order to use SGI to characterise groundwater droughts, given the apparent association between drought duration and m_{max}, it would be helpful to understand the potential controls on SGI autocorrelation. Here two basic potential sources of SGI autocorrelation have been investigated. The first potential source of autocorrelation in SGI is that it arises primarily from autocorrelation in the recharge signal. Precipitation has relatively short significant autocorrelation, as reflected in the comparative SPI and SGI autocorrelation plots, Fig. 7 (top panel). When the precipitation signal passes through the unsaturated zone higher frequency components of the signal may be degraded or filtered out so that when recharge occurs at the groundwater table the recharge signal may have a longer autocorrelation. The second possible cause of autocorrelation in SGI may be associated with saturated storage, drainage and flow processes in the aquifer. It can be postulated that aquifers that are relatively transmissive and/or have relatively low storage may dissipate pulses of recharge more quickly than those with relatively low transmissivity and/or high storage and so may be expected exhibit relatively short SGI autocorrelations and vice versa.

To investigate these potential causes of SGI autocorrelation a simple approach has been adopted that uses readily available information to explore relationships between

HESSD
10, 7537–7574, 2013

m_{max} and two different possible explanatory variables. Estimates of mean unsaturated zone thickness, U, is taken as a surrogate for the potential influence of recharge-related process on m_{max}. In addition, estimates of aquifer properties transmissivity (T), storativity (S) have been used to estimate hydraulic diffusivity, D (T/S), at each site, where D is taken to be a surrogate for the potential influence of intrinsic saturated aquifer properties on m_{max}. Plots of U and log$D$ against m_{max} are given in Fig. 12b and c respectively. For the Chalk and Lincolnshire Limestone aquifers, there appears to be a systematic positive relationship between mean unsaturated zone thickness and m_{max}, but no such relationship appears to hold for the other two aquifers, Fig. 12b. This appears to support the hypothesis that, on the Chalk and Lincolnshire Limestone aquifers at least, the origin of relatively long SGI autocorrelation is associated with recharge process, whether it is by piston flow, by-pass flow or some combination of recharge mechanisms (Price et al., 1993). However, this does not explain why the Permo-Triassic sandstone sites, each with relatively thin unsaturated zones (all less than 10 m), exhibit such long SGI autocorrelations. Another factor must be influencing the SGI autocorrelations at these sites. A plot of log hydraulic diffusivity, log$D$, against m_{max}, Fig. 12c, shows that for all aquifers log$D$ is negatively linearly related to m_{max}. This relationship is particularly pronounced for the granular aquifers such as the Permo-Triassic sandstone and Lower Greensand, but is not evident if just the Chalk and Lincolnshire Limestone sites are considered. These observations appear to support the second hypothesis that, at least for the granular aquifers, longer SGI autocorrelations are associated with aquifers where the hydraulic diffusivity is relatively low.

In summary, it is inferred from Fig. 12 that autocorrelation in SGI and hence groundwater drought phenomena are an aquifer dependent consequence of both autocorrelation in groundwater recharge and of the effect of intrinsic aquifer characteristics on saturated flow and storage. These results highlight the need to take into account the hydrogeological context of groundwater monitoring sites when designing and interpreting data from groundwater level drought monitoring networks.

HESSD
10, 7537–7574, 2013

J. P. Bloomfield and B. P. Marchant

6 Conclusions

- The SPI methodology can be applied to groundwater level data to produce a Standardised Groundwater level Index (SGI) if the SPI methodology is suitably modified to take in to account the form and nature of groundwater level time series.
- Given strong correlations established between SPI and SGI and good agreement of SGI time series with previously independently documented droughts, SGI provides a robust quantification of groundwater drought.
- Maximum cross-correlations between SPI and SGI are associated with a range of SPI accumulations periods that are a function of SGI autocorrelation. In addition, groundwater drought durations defined by SGI time series are also a function of SGI autocorrelation.
- Autocorrelation in SGI appears to be an aquifer dependent function of autocorrelation in groundwater recharge signal and of the effects of intrinsic aquifer properties on saturated groundwater flow and storage.

Acknowledgements. The work described has been funded by the British Geological Survey (Natural Environment Research Council), and this paper is published with the permission of the Executive Director of the British Geological Survey (Natural Environment Research Council).

References

Akaike, H.: Information theory and an extension of the maximum likelihood principle, in: Second International Symposium on Information Theory, edited by: Petrov, B. N. and Csáki, F., Akadémiai Kiadó, Budapest, 267–281, 1973.

Allen, D. J., Brewerton, L. J., Coleby, L. M., Gibbs, B. R., Lewis, M. A., MacDonald, A. M., Wagstaff, S. J., and Williams, A. T.: The physical properties of major aquifers in England and Wales, British Geological Survey Research Report WD/97/34, Keyworth, UK, 1997.

HESSD

10, 7537–7574, 2013

Analysis of groundwater drought using a variant of SPI

J. P. Bloomfield and B. P. Marchant

BADC: Met Office Integrated Data Archive System (MIDAS) Land and Marine Surface Stations Data (1853–current), http://badc.nerc.ac.uk/view/badc.nerc.ac.uk__ATOM__dataent_ukmo-midas, last access: 21 May 2013.

Bloomfield, J. P.: Characterization of hydrogeologically significant fracture distributions in the Chalk: an example from the Upper Chalk of SE England, J. Hydrol., 184, 355–379, 1996.

Bloomfield, J. P., Gooddy, D. C., Bright, M. I., and Williams, P. J.: Pore-throat size distributions in Permo-Triassic sandstones from the United Kingdom and some implications for contaminant hydrogeology, Hydrogeol. J., 9, 219–230, 2001.

Bloomfield, J. P., Allen, D. J., and Griffiths, K. J.: Examining geological controls on baseflow index (BFI) using regression analysis: an illustration from the Thames Basin, UK, J. Hydrol., 373, 164–176, 2009.

Bhuiyan, C., Singh, R. P., and Kogan, F. N.: Monitoring drought dynamics in the Aravalli region (India) using different indices based on ground and remote sensing data, Int. J. Appl. Earth Obs., 8, 289–302, 2006.

Chang, T. J. and Teoh, C. B.: Use of the kriging method for studying characteristics of ground water droughts, J. Am. Water Resour. As., 31, 1001–1007, 1995.

Cole, G. A. and Marsh, T. J.: An historical analysis of drought in England and Wales, in: Climate Variability and Change: Hydrological Impacts, edited by: Demuth, S., Gustard, A., Planos, E., Scatena, F., and Servat, E., International Association of Hydrological Sciences (IAHS) 5th FRIEND World Conference Havana, Cuba, November, 2006, IAHS Publication no. 308, Wallingford, UK, 483–489, 2006.

Diggle, P. J.: Time Series: A Biostatistical Introduction, 1st Edn., Oxford Science Publications/Clarendon Press, Oxford, 1990.

Edwards, D. C. and McKee, T. B.: Characteristics of 20th Century Drought in the United States at Multiple Time Scales, Colorado State University, Climatology Report No. 97–2, Colorado, 1997.

Eltahir, E. A. B. and Yeh, P.J- F.: On the asymmetric response of aquifer water level to floods and droughts in Illinois, Water Resour. Res., 35, 1199–1217, 1999.

Everitt, B. S.: The Cambridge Dictionary of Statistics, 2nd Edn., Cambridge University Press, Cambridge, 2002.

Fink, A. H., Brucher, T., Kruger, A., Leckebush, G. C., Pinto, J. G., and Ulbrich, U.: The 2003 European summer heatwaves and drought – synoptic diagnosis and impacts, Weather, 59, 209–216, 2004.

HESSD
10, 7537–7574, 2013

Analysis of groundwater drought using a variant of SPI

J. P. Bloomfield and B. P. Marchant

Fiorillo, F. and Guadagno, F. M.: Karst spring discharge analysis in relation to drought periods, using SPI, Water Resour. Manage., 24, 1864–1884, 2010.

Fiorillo, F. and Guadagno, F. M.: Long karst spring discharge time series and drought occurrence in Southern Italy, Environ. Earth Sci., 65, 2273–2283, 2012.

Fleig, A. K., Tallaksen, L. M., Hisdal, H., and Hannah, D. M.: Regional hydrological drought in north-western Europe: linking a new regional drought area index with weather types, Hydrol. Process., 25, 1163–1179, 2011.

Hannaford. J., Lloyd-Hughes, B., Keef, C., Parry, S., and Prudhomme, C.: Examining the large-scale spatial coherence of European drought using regional indicators of precipitation and streamflow deficit, Hydrol. Process., 25, 1146–1162, 2010.

Hughes, J. D., Petrne, K. C., and Silberstein, R. P.: Drought, groundwater storage and stream flow decline in southwestern Australia, Geophys. Res. Lett., 39, L03408, doi:10.1029.2011GL050797, 2012.

Keller, V., Young, A. R., Morris, D., and Davies, H.: Continuous Estimation of River Flows (CERF), Technical Report: Estimation of Precipitation Inputs, Environment Agency R&D Project Report WD-101, Centre for Ecology and Hydrology, Wallingford, 2005.

Leblanc, M. J., Tregoning, P., Ramillien, G., Tweed, S. O., and Fakes, A.: Basin-scale, integrated observations of the early 21st century multiyear drought in southeast Australia, Water Resour. Res., 45, W04408, doi:10.1029.2008WR007333 2009.

Lloyd-Hughes, B. and Saunders, M. A.: A drought climatology for Europe, Int. J. Climatol., 22, 1571–1592, 2002.

Marsh, T. J., Cole, G., and Wilby, R.: Major droughts in England and Wales, 1800–2006, Weather, 62, 87–93, 2007.

MATLAB: MATLAB and Statistics Toolbox Release 2012b, The MathWorks, Inc., Natick, Massachusetts, United States, 2012.

Maurice, L. D., Atkinson, T. C., Barker, J. A., Bloomfield, J. P., Farrant, A. R., and Williams, A. T.: Karstic behaviour of groundwater in the English Chalk, J. Hydrol., 330, 63–70, 2006.

McEvoy, D. J., Huntington, J. L., Abatzoglou, J. T., and Edwards, L. M.: An evaluation of multiscalar drought indices in Nevada and eastern California, Earth Interact., 16, 1–8, doi:10.1175/2012EI000447.1, 2012.

McKee, T. B., Doesken, N. J., and Leist, J.: The relationship of drought frequency and duration time scales, 8th Conference on Applied Climatology, 17–22 January 1993, Anaheim, California, 179–184, 1993.

Mendicino, G., Senatore, A., and Versace, P.: A Groundwater Resource Index (GRI) from drought monitoring and forecasting in a Mediterranean climate, J. Hydrol., 357, 282–302, 2008.

Mishra, A. K. and Singh, V. P.: A review of drought concepts, J. Hydrol., 391, 202–216, 2010.

Nalbantis, I. and Tsakiris, G.: Assessment of hydrological drought revisited, Water Resour. Manage., 23, 881–897, 2009.

National Groundwater Level Archive: http://www.ceh.ac.uk/data/nrfa/data/ngla.html, last access: 21 May 2013.

National River Flow Archive: The 2004–2006 Drought – and outlook for 2007, http://www.nwl.ac.uk/ih/nrfa/water_watch/dr2004_06/index.html, last access: 21 May 2013.

Osti, A. L., Lambert, M. F., and Metcalfe, A. V.: On spatiotemporal drought classificationin New South Wales: development and evaluation of alternative techniques, Aust. J. Water Resour., 12, 21–34, 2008.

Panu, U. S. and Sharma, T. A.: Challenges in drought research: some perspectives and future directions, Hydrolog. Sci. J., 47, S19–S30, 2000.

Peters, E., Torfs, P. J. J. F., van Lanen, H. A. J., and Bier, G.: Propagation of drought through groundwater – a new approach using linear reservoir theory, Hydrol. Process., 17, 3023–3040, 2003.

Peters, E., van Lanen, H. A. J., Torfs, P. J. J. F., and Bier, G.: Drought in groundwater – drought distribution and performance indicators, J. Hydrol., 306, 302–317, 2005.

Peters, E., Bier, G., van Lanen, H. A. J., and Torfs, P. J. J. F.: Propagation and spatial distribution of drought in a groundwater catchment, J. Hydrol., 321, 257–275, 2006.

Price, M., Downing, R. A., and Edmunds, W. M.: The Chalk as an aquifer, in: The Hydrogeology of the Chalk of North-West Europe, edited by: Downing, R. A., Price, M., and Jones, G. P., Clarendon Press, Oxford, UK, 14–34, 1993.

Santos, M. A.: Regional droughts: a stochastic characterisation, J. Hydrol., 66, 183–211, 1983.

Sheffield, J. and Wood, E. F.: Global trends and variability in soil moisture and drought characteristics, 1950–2000, from observation – driven simulations of the terrestrial hydrologic cycle, J. Climate, 21, 432–458, 2008.

Shulka, S. and Wood, A. W.: Use of a standardized runoff index for characterizing hydrologic drought, Geophys. Res. Lett., 35, L02405, doi:10.1029/2007GL032487, 2008.

HESSD
10, 7537–7574, 2013

Analysis of groundwater drought using a variant of SPI

J. P. Bloomfield and B. P. Marchant

Tallaksen, L. M. and van Lanen, H. A. J.: Hydrological drought. Processes and Estimation Methods for Streamflow and Groundwater, Developments in Water Sciences 48, Elsevier, the Netherlands, 2004.
Tallaksen, L. M., Hisdal, H., and van Lanen, H. A. J.: Propagation of Drought in a Groundwater Fed Catchment, the pang in the UK in Climate Variability and Change: Hydrological Impacts, edited by: Demuth, S., Gustard, A., Planos, E., Scatena. F., and Servat, E., International Association of Hydrological Sciences (IAHS) 5th FRIEND World Conference Havana, Cuba, November 2006, IAHS Publication no. 308, Wallingford, UK, 128–133, 2006.
Tallaksen, L. M., Hisdal, H., and van Lanen, H. A. J.: Space-time modelling of catchment scale drought characteristics, J. Hydrol., 375, 363–372, 2009.
Thompson, N., Barrie, I. A., and Ayles, M.: The Meteorological Office Rainfall and Evaporation Calculation System (MORECS), Hydrological Memorandum 45, Met. Office, Bracknell, UK, 1981.
van Lanen, H. A. J. and Tallaksen, L. M.: Hydrological drought, climate variability and change, in: Climate and Water, edited by: Heinonen, M., Proceedings of the Third International Conference on Climate and Water, Helsinki, Finland, 3–6 September, Finnish Environment Institute (SYKE), 488–493, 2007.
Vincente-Serrano, S. M. and Lopez-Moreno, J. I.: Hydrologic response to different time scales of climatological drought: an evaluation of the standardized precipitation index in a mountainous Mediterranean basin, Hydrogeol. Earth Syst. Sci., 9, 523–533, 2005.
Vincente-Serrano, S. M., Begueria, S., and Lopez-Moreno, J. I.: A multiscalar drought index sensitive to global warming: the standardized precipitation evapotranspiration index, J. Climate, 23, 1696–1718, 2010.
Wilhite, D. A.: Drought as a natural hazard: concepts and definitions, in: Drought: A Global Assessment, edited by: Wilhite, D. A., Natural Hazards and Disasters Series, Routledge Publishers, London, 3–18, 2000.
Wu, H., Hayes, M. J., Wilhite, D. A., and Svoboda, M. A.: The effect of the length of record on the standardized precipitation index calculation, Int. J. Climatol., 25, 205–520, 2005.

HESSD
10, 7537–7574, 2013

Analysis of groundwater drought using a variant of SPI

J. P. Bloomfield and B. P. Marchant

Table 1. Summary information for the 14 groundwater level hydrographs and associated rainfall data for each site.

Site	Aquifer	Start of record	End of record	Mean annual precipitation (mm)	Well depth (m)	Groundwater level (m a.s.l.) Min.	Max.	Mean	Mean unsaturated zone (m)	Transmissivity ($m^2 day^{-1}$)	Storage coefficient	Log_{10} Hydraulic Diffusivity
1. Ashton Farm	Chalk	1 Mar 1974	1 Jan 2006	1010	11.70	63.13	71.46	67.55	4.57	210	0.003	4.85
2. Bussels No. 7	Permo-Trias Sandstone	1 Dec 1971	1 Jan 2006	800	91.44	22.91	25.28	23.89	3.07	95	0.1	2.98
3. Chilgrove House	Chalk	1 Jan 1900	1 Jan 2006	950	62.03	33.46	76.24	48.89	28.28	500	0.002	5.40
4. Dalton Holme	Chalk	1 Feb 1909	1 Jan 2006	740	28.50	10.19	23.76	17.15	17.38	1260	0.007	5.24
5. Heathlanes	Permo-Trias Sandstone	1 Aug 1970	1 Jan 2006	660	8.74	60.25	64.45	62.01	6.60	200	0.1	3.30
6. Little Bucket Farm	Chalk	1 Jan 1973	1 Jan 2006	820	31.33	56.77	86.94	68.35	18.94	720	0.003	5.38
7. Llanfair DC	Permo-Trias Sandstone	1 Feb 1972	1 Jan 2006	820	121.90	78.67	81.18	79.83	3.23	130	0.1	3.11
8. Lower Barn Cottage	Lower Greensand	1 Apr 1977	1 Jan 2006	840	8.25	10.14	13.49	11.06	6.95	1000	0.02	4.70
9. New Red Lion	Lincolnshire Limestone	1 Sep 1964	1 Jan 2006	610	50.00	3.37	23.35	14.08	19.39	2750	0.05	4.74
10. Rockley	Chalk	1 Mar 1935	1 Jan 2006	810	17.60	128.65	143.87	134.52	12.06	620	0.006	5.01
11. Stonor Park	Chalk	1 Jun 1961	1 Jan 2006	800	87.50	61.55	92.05	75.51	45.91	820	0.004	5.31
12. Therfield Rectory	Chalk	1 Jun 1956	1 Jan 2006	580	83.23	71.50	96.53	80.37	74.55	670	0.004	5.22
13. Well House Inn	Chalk	1 Nov 1942	1 Jan 2006	820	50.60	83.54	104.19	95.36	37.00	720	0.003	5.38
14. West Dean No. 3	Chalk	1 May 1940	1 Jan 2006	810	24.99	1.06	4.85	1.84	11.65	500	0.002	5.40

HESSD
10, 7537–7574, 2013

Table 2. Value of the maximum cross-correlation between SPI and SGI, SGI autocorrelation range (m_{max}), the accumulation period associated with maximum cross-correlation between SPI and SGI (q_{max}), the lag associated with maximum cross-correlation between SPI and SGI (lag_{max}), and maximum and median drought duration at each site.

Site	Cross-correlation	m_{max} (months)	q_{max} (months)	lag_{max} (months)	Maximum drought duration (months)	Median drought duration (months)
1. Ashton Farm	0.72	4	6	0	12	3.5
2. Bussels No. 7	0.83	19	9	0	41	3
3. Chilgrove House	0.74	6	6	0	31	3
4. Dalton Holme	0.76	8	10	0	65	5
5. Heathlanes	0.74	24	28	0	64	2.5
6. Little Bucket Farm	0.87	8	10	1	47	4
7. Llanfair DC	0.79	28	25	0	72	3
8. Lower Barn Cottage	0.81	14	15	0	59	2
9. New Red Lion	0.83	9	8	0	53	3
10. Rockley	0.74	6	7	0	32	4
11. Stonor Park	0.79	11	21	1	48	6
12. Therfield Rectory	0.77	15	21	2	61	9
13. Well House Inn	0.78	10	12	0	49	11
14. West Dean No. 3	0.70	12	7	0	23	2

HESSD
10, 7537–7574, 2013

Table 3. Summary of the major droughts in England from 1900 to the 2006 (after Marsh et al., 2007 and National River Flow Archive, 2011).

Period	Drought characteristics
1890 to 1910	Known as the "Long drought". A major drought with major and sustained groundwater impacts including more intense phases in 1902 and 1905.
1921 to 1922	Severe drought across East Anglia and SE England, but only episodic in NW England.
1933 to 1934	Intense drought across southern England. Major surface water impacts in 1933 with groundwater impacts in 1934.
1959	Three season drought that was most severe in eastern, central and NE England, but only modest groundwater impacts.
1976	Benchmark drought in UK. Severe impacts on river flow and groundwater across UK.
1990 to 1992	Major drought leading to exceptionally low groundwater levels in summer 1992, with probably lowest for at least 90 yr.
1995 to 1997	Long duration drought with intense episodes. Initial surface water stress followed by very depressed groundwater levels particularly associated with hot summer in 1995.

HESSD
10, 7537–7574, 2013

J. P. Bloomfield and B. P. Marchant

Title Page
Abstract Introduction
Conclusions References
Tables Figures
Back Close
Full Screen / Esc
Printer-friendly Version
Interactive Discussion

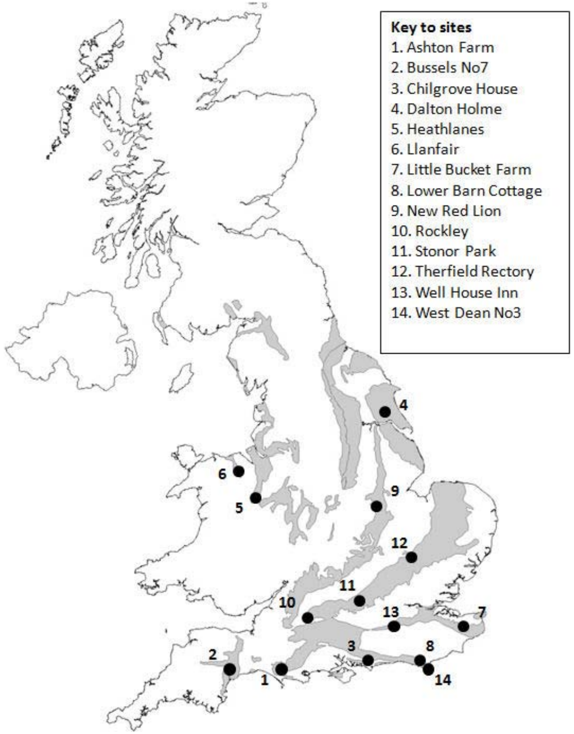

Fig. 1. Location of the observation boreholes in relation to the major aquifers in the UK.

HESSD
10, 7537–7574, 2013

Analysis of groundwater drought using a variant of SPI

J. P. Bloomfield and B. P. Marchant

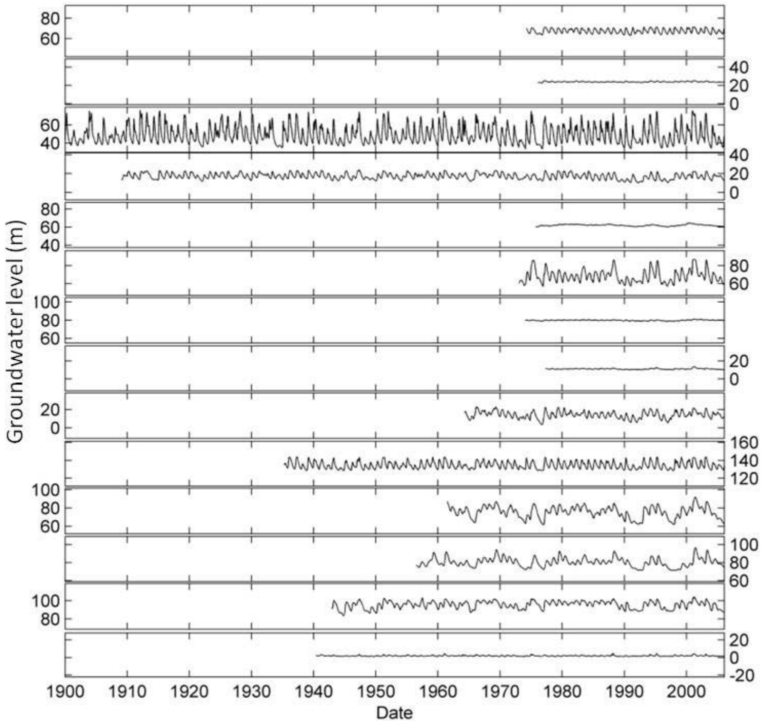

Fig. 2. Groundwater level hydrographs for the 14 study sites. Plots are for sites listed in Table 1 in alphabetical order from top to bottom.

HESSD
10, 7537–7574, 2013

J. P. Bloomfield and B. P. Marchant

Title Page
Abstract Introduction
Conclusions References
Tables Figures
◂◂ ▸▸
◂ ▸
Back Close
Full Screen / Esc
Printer-friendly Version
Interactive Discussion

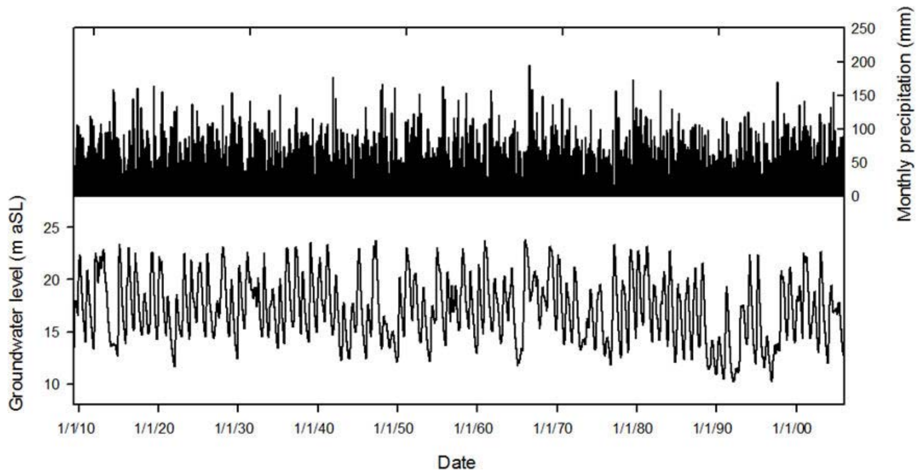

Fig. 3. Time series showing monthly precipitation totals (one month aggregation) and corresponding monthly groundwater level hydrograph for Dalton Holme from 1909 to 2005.

HESSD
10, 7537–7574, 2013

Analysis of groundwater drought using a variant of SPI

J. P. Bloomfield and B. P. Marchant

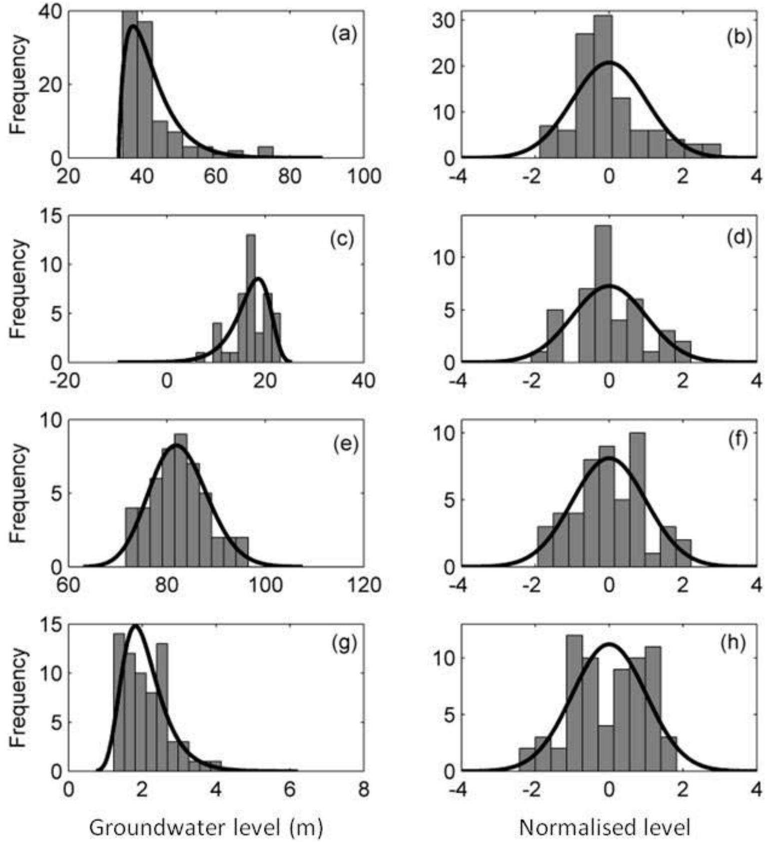

Fig. 4. Examples of histograms of groundwater levels and best fitting parametric distributions (**a**, **c**, **e** and **g**), and corresponding histograms of normalized values and standardized normal distribution for groundwater level data (**b**, **d**, **f** and **h**) from Chilgrove House in November, New Red Lion in April, Therfield Rectory in May, and West Dean No. 3 in June respectively.

HESSD
10, 7537–7574, 2013

J. P. Bloomfield and B. P. Marchant

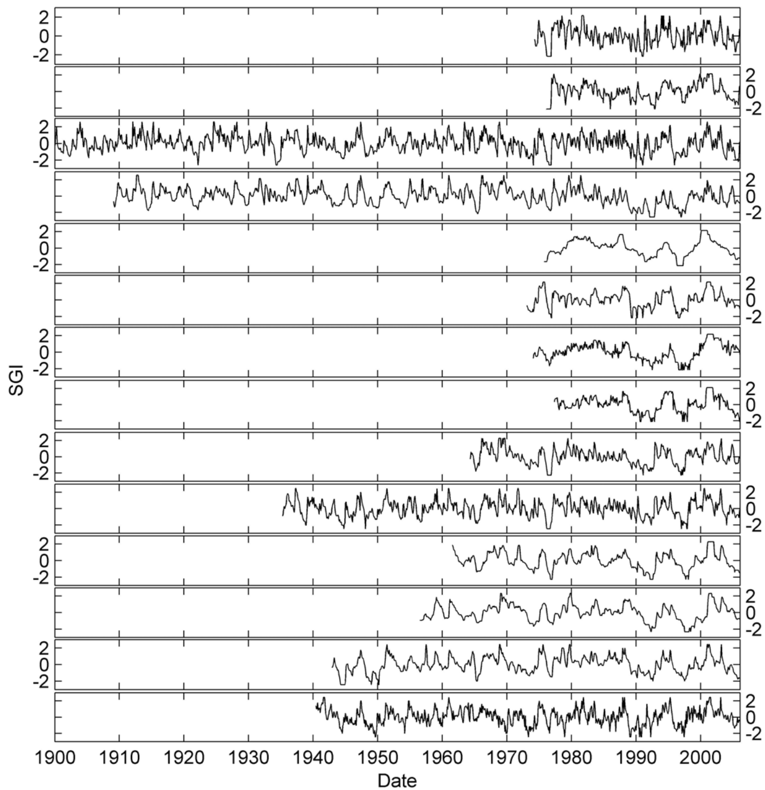

Fig. 5. Calculated time series of SGI for the 14 sites. Plots are for sites listed in Table 1 in alphabetical order from top to bottom.

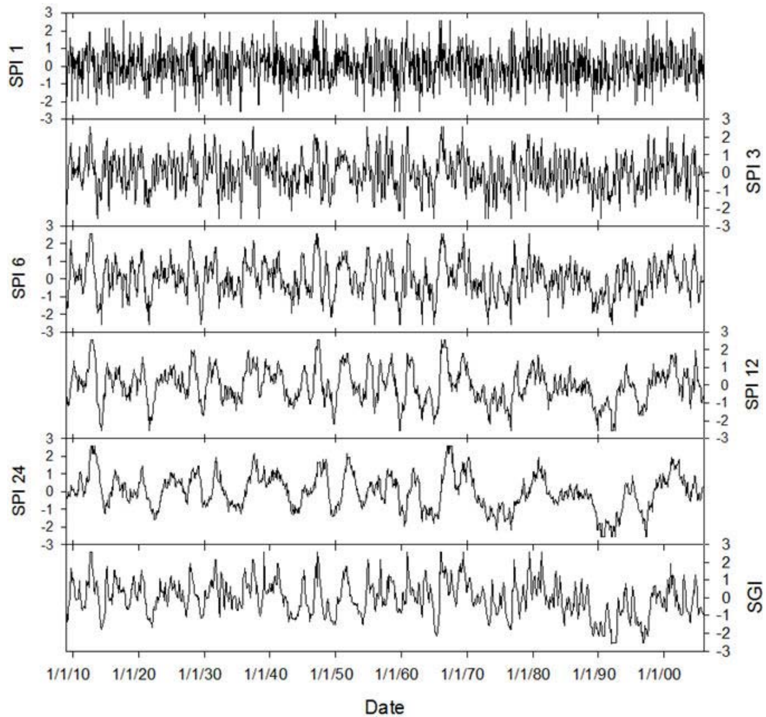

Fig. 6. SPI for Dalton Holme for accumulation periods q = 1, 3, 6, 12 and 24 and corresponding SGI.

HESSD
10, 7537–7574, 2013

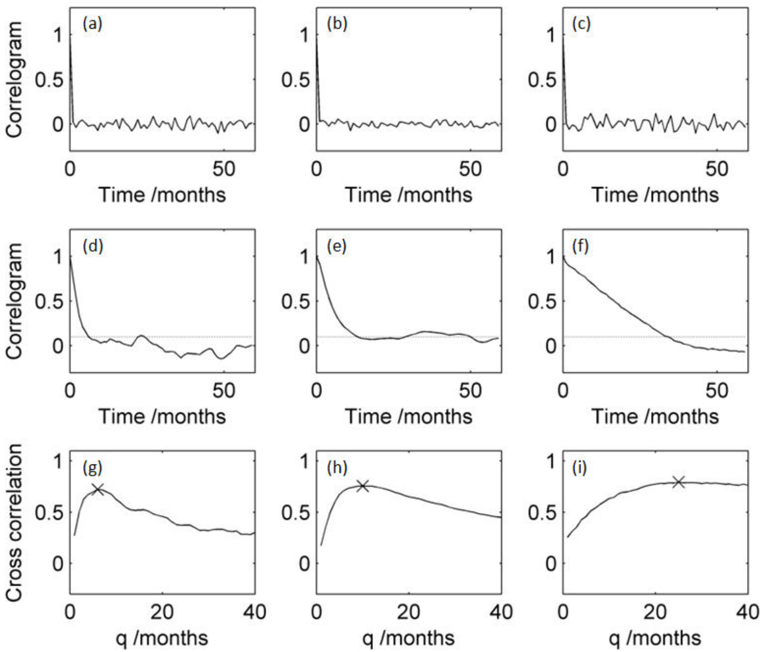

Fig. 7. (a)–(c) SPI autocorrelation as a function of lag in months for Ashton Farm (left), Dalton Holme (centre) and Llanfair (right), **(d)–(f)** SGI autocorrelation as a function of lag in months for the corresponding sites, where the dashed line is the SGI autocorrelation threshold, t_{SGI}, and **(g)–(i)** cross-correlation between SGI and SPI as a function of SPI accumulation period in months for the corresponding sites.

HESSD
10, 7537–7574, 2013

Analysis of groundwater drought using a variant of SPI

J. P. Bloomfield and B. P. Marchant

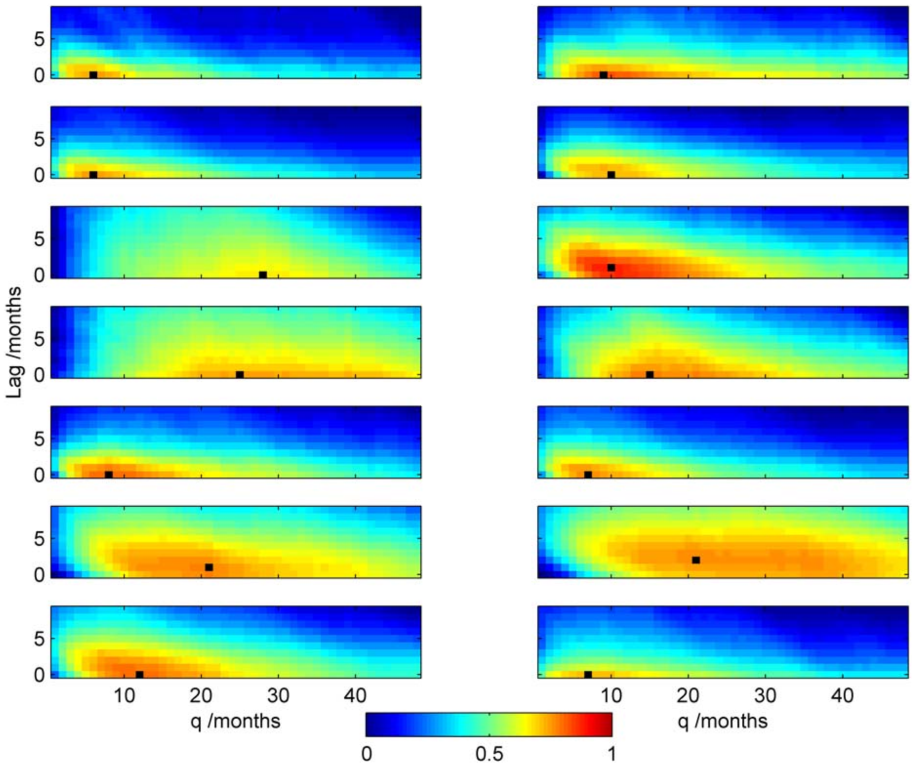

Fig. 8. Heat map of showing the variation in cross-correlation co-efficient between SPI and SGI as a function of SPI precipitation accumulation period, q, and lag between SPI and SGI time series. The maximum correlation for each accumulation period is been highlighted (black cell). The heat maps are for sites listed in Table 1 in alphabetical order from top left to bottom right.

HESSD
10, 7537–7574, 2013

Analysis of groundwater drought using a variant of SPI

J. P. Bloomfield and B. P. Marchant

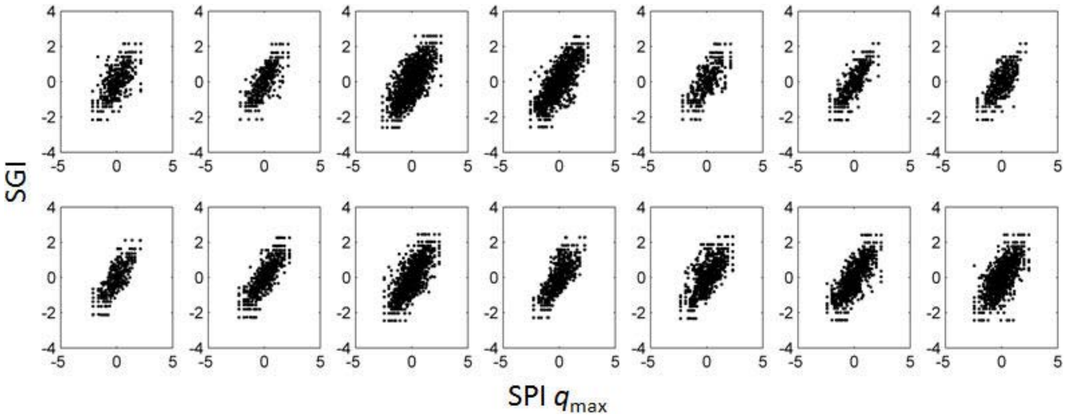

Fig. 9. SGI as a function of SPI q_{max} for each site. The plots are for sites listed in Table 1 in alphabetical order from top left to bottom right.

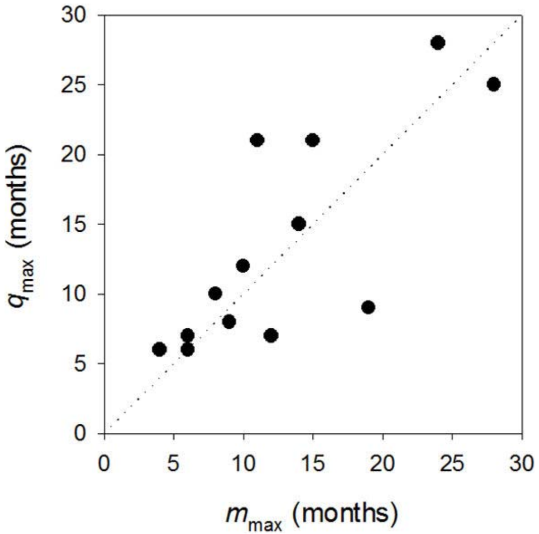

Fig. 10. Plot of the SPI precipitation accumulation period, q_{max}, against autocorrelation range, m_{max}, associated with the maximum cross-correlation between SPI and SGI for all study sites. A 1 : 1 line is shown for reference.

HESSD
10, 7537–7574, 2013

Analysis of groundwater drought using a variant of SPI

J. P. Bloomfield and B. P. Marchant

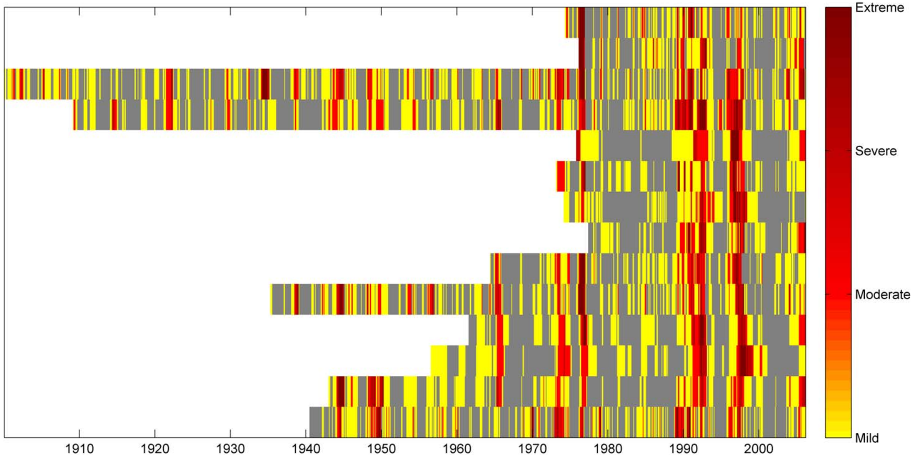

Fig. 11. Monthly values of SGI for the 14 sites as heat map.

HESSD
10, 7537–7574, 2013

Analysis of groundwater drought using a variant of SPI

J. P. Bloomfield and B. P. Marchant

HESSD
10, 7537–7574, 2013

Analysis of groundwater drought using a variant of SPI

J. P. Bloomfield and B. P. Marchant

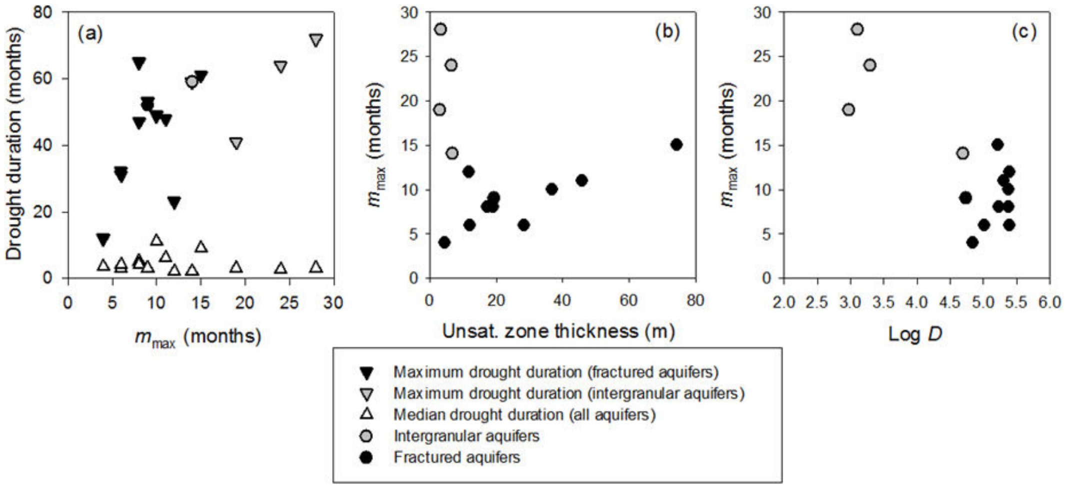

Fig. 12. (a) Maximum and median drought durations at each site as a function of m_{max}, and m_{max} as a function of **(b)** unsaturated zone thickness and **(c)** log hydraulic diffusivity.